

X-690-73-366

PREPRINT

NASA TM X-70542

MAGNETOSPHERIC MAPPING WITH QUANTITATIVE GEOMAGNETIC FIELD MODELS

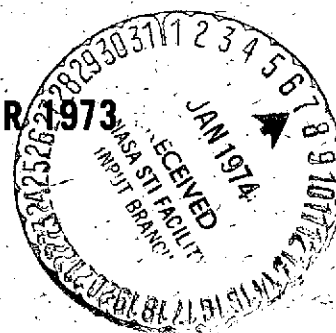
(NASA-TM-X-70542) MAGNETOSPHERIC MAPPING
WITH QUANTITATIVE GEOMAGNETIC FIELD MODELS
(NASA) 37 p HC \$4.00 CSCL 04A

N74-13097

Unclas
G3/13 24653

DONALD H. FAIRFIELD
GILBERT D. MEAD

DECEMBER 1973



GSFC

GODDARD SPACE FLIGHT CENTER
GREENBELT, MARYLAND

MAGNETOSPHERIC MAPPING WITH QUANTITATIVE
GEOMAGNETIC FIELD MODELS

Donald H. Fairfield
Laboratory for Extraterrestrial Physics

and

Gilbert D. Mead
Laboratory for Space Physics

NASA Goddard Space Flight Center
Greenbelt, Maryland 20771

December, 1973

1

Abstract

The Mead-Fairfield geomagnetic field models have been used to trace field lines between the outer magnetosphere and the earth's surface. The results are presented in terms of ground latitude and local time contours projected to the equatorial plane and into the geomagnetic tail. With these contours various observations can be mapped along field lines between high and low altitudes. Low altitudes observations of the polar cap boundary, the polar cusp, the energetic electron trapping boundary and the sunward convection region are projected to the equatorial plane and compared with the results of the model and with each other. The results provide quantitative support to the earlier suggestions that the trapping boundary is associated with the last closed field line in the sunward hemisphere, the polar cusp is associated with the region of the last closed field line, and the polar cap projects to the geomagnetic tail and has a low latitude boundary corresponding to the last closed field line. The sunward convection region is associated with most of the magnetosphere outside the plasmopause, but whether the region extends all the way outward to the last closed field line or inward to the

plasmopause is uncertain. Field lines from $6.6 R_E$ in the geomagnetic equatorial plane intersect the earth between 67.4° and 65.1° , with the exact value depending on the dipole tilt angle, season, local time and geomagnetic activity.

Introduction

Field and particle observations made along high latitude geomagnetic field lines form the basis for our current understanding of magnetosphere processes. Such measurements have generally been made either within $1 R_E$ of the earth's surface or at large distances near the equatorial plane. It is important to compare measurements in these two regions because the effects observed in one region may be controlled by physical processes in the other region. Since most observed magnetosphere processes are related to charged particles which follow geomagnetic field lines, it is especially necessary to have accurate knowledge of the geomagnetic field in order to map the observed phenomena along field lines from one region to another. Within approximately $5 R_E$ of the earth a dipole model is usually adequate for such mapping purposes, but at greater distances, where external perturbations become larger relative to the internal field, models including these external sources must be used.

A companion paper (Mead and Fairfield, 1973) presents four such field models which have been derived from over

4000 hours of vector magnetic field data obtained by four Explorer spacecraft. The present paper will present results obtained from these models by tracing the field lines between the earth's surface and their intersection with either the equatorial plane or a cross section of the geomagnetic tail. Various statistical results obtained from low-altitude polar-orbiting spacecraft will be projected to the outer magnetosphere. This procedure will demonstrate use of the mapping technique and at the same time allow the earlier results to be viewed in a different context which may yield greater insight into physical processes. The low altitude measurements will be found to map to those regions of the magnetosphere that would be expected on the basis of various theoretical speculations. This fact can therefore be viewed as providing quantitative support for the theoretical expectations. Alternatively, one could accept the validity of the theoretical ideas and argue that the mapping supports the accuracy of the new quantitative field models. Small differences between the projected experimental results and the expectations of various theories point out some critical outstanding questions of magnetospheric physics.

Field Line Tracing

The work of Mead and Fairfield has produced four independent models corresponding to geomagnetic conditions that are quiet ($K_p < 2$), disturbed ($K_p \geq 2$), super-quiet ($K_p \leq 0^+$), and super-disturbed ($K_p \geq 3$). Each of the models consists of a set of coefficients in a power series expansion for the disturbance field as a function of the position variables (solar magnetic coordinates) X, Y, and Z and tilt angle (the geomagnetic latitude of the sun). The disturbance field when added to a dipole field yields a realistic magnetic field at any point in space and for any tilt angle. The range of validity for the models is restricted to distances $< 17 R_E$ and the models have imposed north-south symmetry and also east-west symmetry about a line 4° west of the sun, (ie. there is perfect north-south and east-west symmetry for zero tilts and for positive tilts the northern hemisphere has the same configuration as the southern hemisphere does for negative tilts). It is important to realize that even though field models are available for four different K_p ranges, the models are static, whereas, the actual magnetospheric configuration is dynamic and

often undergoes large changes on a time scale of tens of minutes. For this reason, the models are primarily of use in mapping phenomena where time variations have been averaged out.

Since the magnetic field is available at all points of space, it is possible to trace field lines using any of the four models. Figure 1 presents some results obtained by tracing field lines and compares differences between the four models. At the top of Figure 1 is the equatorial crossing distance of the outermost closed field line in the noon meridian for zero tilt angles for each of the four models. The values range from 12.2 in the super-quiet model to 10.4 in the super-disturbed model. It should be emphasized that these values emerge directly from the best fit models, in contrast to most earlier magnetospheric field models, where this distance is an adjustable parameter. The agreement with an observed magnetopause distance (Fairfield, 1971) of $10.9 R_E$ is quite good, especially since the observed values include all tilt angles; the effect of non-zero tilts is to move the last closed field lines in the model closer to the earth. Figure 1 supports the common assumption that the

magnetopause corresponds to the last closed field line on the dayside of the earth.

In the lower portion of Figure 1, the latitude where the last closed field line in the noon meridian plane intersects the earth is plotted for the four models. These values range from 80.5° at low K_p to 76.2° at high K_p , which may be contrasted with the results of theoretically-derived field models (Williams and Mead, 1965; Choe and Beard, 1973; see Roederer, 1969), which are generally greater than 80° with realistic input parameters. The surface latitude of the last closed field line from the equatorial plane is independent of longitude in the solar hemisphere for any of the models. Thus the calculations support the concept (e.g. Aubry et al., 1970; Fairfield and Ness, 1970) that some lines of force that close on the day side of the earth under quiet conditions extend into the geomagnetic tail under disturbed conditions. The results are also consistent with those of Burch (1972) who found that the latitude of the cusp at low altitudes moves equatorward in association with a southward interplanetary field, which in turn is known to correlate well with K_p .

Additional results from tracing three dimensional field lines are presented in Figure 2 (quiet model) and Figure 3 (disturbed model). These figures attempt to consolidate three dimensional information in a two dimensional figure by taking latitude and local time points on the earth's surface and tracing the corresponding field lines to the outer magnetosphere. The bottom portion of the figures show the intersection of these field lines with the equatorial plane, while the upper portions show their intersection with a cross section of the tail at $X = -10 R_E$. At 60° , where perturbations are small compared to the internal field, the latitude contours project approximately as circles, but at higher latitudes deviations from circularity increase. In Figure 2 the 69° latitude field line from midnight crosses the equatorial plane near $X = -10 R_E$ with higher latitude field lines crossing the $X = -10 R_E$ plane and going into the tail. For the disturbed model (Figure 3) the 69° field line goes further into the tail. The models are probably deficient at the larger Y values in Figures 2 and 3 at distances which exceed the $17 R_E$ limit of the original data. At these large distances the

Z component of the model field in the equatorial plane begins increasing in magnitude in a manner for which there is no observational support (Mead and Fairfield, 1973). The X axis in Figures 2 and 3 are aligned along the earth-sun direction and the east-west asymetry is due to the fact that the model is symetric about a direction 4° from the earth sun line.

Mapping Low Altitude Measurements

Figures 2 and 3 and their equivalents for the other 2 models can be used for mapping various low altitude measurements to the outer magnetosphere. Winningham (1972) used low altitude plasma measurements to determine the upper and lower boundaries of the polar cusp as a function of longitude for various K_p ranges. Evans and Stone (1972) deduced the boundary of the polar cap by determing the low latitude termination to the polar cap access region for > 530 Kev solar electrons for two K_p ranges. If the arguments are valid that (1) the low energy polar cusp plasma has easy access to the magnetosphere on field lines that enter the magnetosheath and, (2) energetic electrons have access to open tail field lines in the downstream region,

these boundaries ought to be similar and compare favorably to the last closed field line determinations of the model. In Figure 4 the low altitude determinations of the polar cusp and the polar cap (the Evans and Stone measurements were averaged in two-hour local time intervals) during high K_p periods are projected to the outer magnetosphere along the field lines of the super-disturbed model. The polar cusp which is observed in the 9:00 to 16:00 local time region is seen to project partially to closed field lines near the magnetopause and partially to the boundary of the geomagnetic tail (See also Akasofu et al., 1973). The polar cap projects into the geomagnetic tail and actually overlaps the polar cusp to some extent, but no attempt has been made to overlay the two shadings. The low latitude boundary of the polar cap corresponds to the polar cusp region as well as could be expected considering the statistical uncertainties in the boundary determinations and the fact that the K_p ranges are somewhat different. Both the cusp and the polar cap boundary data compare favorably with the predictions of the model. It is also interesting to note that the shape of the low latitude

polar cap boundary projected on the tail cross section corresponds very well to the high latitude boundary of the plasma sheet at $17 R_E$ (Bame et al., 1967).

Figure 5 shows data similar to those of figure 4, only figure 5 is for low K_p conditions and the projection is entirely into the equatorial plane. Again the polar cusp region is designated by shading but now the low latitude boundary of the polar cap is indicated by open circles.

The additional data in figure 5 are those of McDiarmid and Burrows (1968). These authors were able to define two > 35 Kev electron boundaries in the auroral region and determine their average latitudinal position as a function of local time. The higher latitude boundary was defined as the position where flux levels reached background level. They suggested that this "background" boundary should be associated with the last closed field line of the magnetosphere. A lower latitude "smooth" boundary was defined as the location separating a low latitude region of stable fluxes from a higher latitude region of variable fluxes. They suggest that particles

equatorward of this boundary were completing longitudinal drift paths around the earth, whereas particles poleward of this boundary were undergoing pitch angle diffusion. The radial lines in Figure 5 represent equatorial plane projections of the model field lines corresponding to the boundaries of McDiarmid and Burrows. The solid lines represent field lines at the smooth boundary and the dashed lines those of the background boundary. The outer boundary in Figure 5 is the last closed field line of the quiet model and the inner oval is an average plasmopause of Chappell et al., (1971).

The agreement among the various types of data is quite good considering the uncertainties in the data. However, the polar cusp is entirely on closed field lines in figure 5 and the last closed field lines of McDiarmid and Burrows lie somewhat inside of the last closed field lines of the model. It should be noted, however, that the model

field used corresponds to an average K_p of 1 and if a slightly higher K_p model corresponding better to the particle data had been available, more field lines would have gone into the tail (see Figure 1) and the agreement with the particle data would be improved. It should also be noted that the models have been used for zero tilt angle whereas the particle data comes from a variety of tilt angles. If non-zero tilt angles had been used in the model, fewer field lines would have closed on the day side and the agreement with the particle data would have been improved. It is interesting to note that there is a large dawn-dusk asymmetry in the trapping boundary of McDiarmid and Burrows, but only a very small asymmetry in the Evans and Stone data. A similar background field boundary of Fritz (1970) determined in a manner similar to that of McDiarmid and Burrows also did not show a large dawn-dusk asymmetry and it extended to somewhat higher latitude, presumably due to choice of a lower background flux level. Asymmetries in the field model were precluded by imposing east-west symmetry on the model. Figure 5 also implies that energetic solar electrons have access to

field lines which close as near the earth as $17 R_E$. It should be pointed out, however, that the model's validity can be questioned in this region (Mead and Fairfield, 1973) and that a small change in the model could make this field line closing at $17 R_E$ extend many tens of earth radii into the tail.

It should also be noted that Feldstein and Starkov (1970) suggest that the low latitude boundary of the auroral oval was associated with the > 35 Kev background boundary of McDiarmid and Burrows. This observation is consistent with the results of Frank and Gurnett (1971), which associate auroral arcs with "inverted V" particle events which occur at and above the > 45 Kev trapping boundary. These results imply that aurora occur on "open" field lines, where the term "open" is defined in an operational sense in terms of the inability to support bouncing ~ 40 Kev electrons. The component of flux across the neutral sheet probably doesn't go to zero near $20 R_E$ (e.g. Behannon, 1970) so it is likely that aurora actually occur on field lines that cross the neutral sheet at greater distances down the tail.

Low altitude measurements of high latitude electric fields are a particularly interesting phenomena to project

to the equatorial plane since they are due to plasma motions in the outer magnetosphere. Heppner (1972a) obtained measurements near the dawn-dusk meridian and Cauffman and Gurnett (1972) have presented data from a greater range of local times but from an experiment of somewhat lower sensitivity. Although the measurements are of only one electric field component, both groups support a picture of sunward convection within the magnetosphere. When the effects of corotation are neglected and the low altitude measurements are projected to the equatorial plane they appear as in Figure 6. In this figure the two types of shading indicate the two data sets and the arrows the approximate direction of the convection. Also included is the projection of the Harang discontinuity (Harang, 1946) which has been suggested as the ionospheric locus along which occur the initial sudden magnetic field changes indicating the onset of expansion phases of magnetospheric substorms (Heppner, 1972c).

The inner boundary of the convection region is slightly closer to the earth for the data of Heppner, presumably due to greater sensitivity. Whether the convection region really

extends in as far as the plasmopause on a case-by-case basis is an important question which will have to be studied further.

Another important question is whether the day side high latitude boundary of the convection region extends all the way to the magnetopause as proposed by Gurnett and Frank (1973) or whether anti-solar convection exists on closed field lines inside the magnetopause as is indicated in Figure 6. This important question will have to be resolved by direct measurements in the outer magnetosphere. Such anti-sunward convection inside the apparent magnetopause and near the equatorial plane has been observed under special circumstances on ATS-1 (Freeman et al., 1968) and IMP-6 (Heppner, 1972b), but the generality of these observations has not been demonstrated. Recently Hones et al. (1972) and Akasofu et al. (1973) have observed anti-solar convection slightly to the nightside of the dawn-dusk meridian plane, with Vela satellites. This convection region is most prominent at higher latitudes but the lack of corresponding magnetic field measurements makes it particularly difficult to say if the convection occurs on open or closed field lines. Gurnett and Frank (1973)

also find that the high latitude boundary of sunward convection generally coincides with the high latitude termination of > 45 Kev electrons. Comparing McDiarmid and Burrows statistical > 35 Kev electrons boundary (Figure 5) with the Cauffman and Gurnett data of Figure 6 does not reveal any large discrepancies which cannot be explained by statistical uncertainties in the data.

Field Tracing at $6.6 R_E$

Figure 7 presents results obtained by tracing field lines from the synchronous satellite orbit at $6.6 R_E$ in the solar magnetic equatorial plane. The data points indicate the geomagnetic latitudes where field lines originating at hourly intervals in the equatorial plane intersect the earth's surface. Three curves are shown for each model corresponding to a 30° tilt angle and tracing to the summer and winter hemispheres and a 0° tilt angle and tracing to either hemisphere. It can be seen that the surface latitude of field lines from the $6.6 R_E$ orbit exhibit a variation with an amplitude which depends on the tilt angle and the season. The variation is largest in the summer for the most disturbed model (peak to peak amplitude of 2.3°) and smallest in the winter for the quietest model (peak to

peak amplitude of $.3^{\circ}$). It should be pointed out, however, that the curves of Figure 7 are not actual diurnal variations, since on any given day the tilt angle will vary whereas Figure 7 is plotted for a fixed tilt angle. The fact that the three points for each hour do not necessarily fall on a vertical line at the hour indicates that the longitude of the earth intersection also depends on the tilt angle.

The horizontal lines at 67.1° in Figure 7 represent the equivalent results for a dipole field. The maximum latitudes occur near noon where solar wind compression causes a field line from a higher latitude to intersect the $6.6 R_E$ orbit. At other longitudes the field is more stretched out, causing lower latitude field lines to intersect this location. The fact that most of the points fall below the dipole value indicates that at most longitudes the ring current effects, causing inflated field lines, predominate over the compression effects of the solar wind.

Summary and Discussion

In summarizing the above results it can be said that there is general agreement between the predictions of the models and the particle measurements and their interpretation.

Specifically, the polar cap as determined from low altitude solar electron measurements projects to the geomagnetic tail and its low latitude boundary is close to the location of both the polar cusp and the limit of trapped > 35 Kev electrons. The polar cusp and the background trapping boundary correspond closely to the last closed field lines of the models. This fact is particularly significant since older field models generally give higher latitudes for last closed field lines and hence would not be in such good agreement with the particle data. All phenomena have a similar variation with magnetic activity which are consistent with the transport of flux to the tail under disturbed conditions. The region of sunward convection as determined from low altitude measurements corresponds to almost the entire volume of the magnetosphere outside the plasmapause, but whether its boundaries extend all the way to the last closed field line or the plasmapause cannot be reliably determined from the available data.

The general agreement between the prediction of the model and the results of particle measurements suggest that there are probably no grossly unrealistic features in the

field model and that there has been no serious misinterpretation of the particle data. More detailed comparisons between model predictions and magnetosphere measurements could, in principle, be used to answer many fundamental questions of magnetospheric physics. It would be interesting to know if polar cusp plasma resides entirely on field lines which enter the magnetosheath or whether the regions designated by Winningham (1972) include particles that have diffused onto closed field lines, as has been suggested by Gurnett and Frank (1973). It is important to know if anti-solar convection exists on closed field lines inside the magnetopause in order to understand physical processes at the magnetopause. Determination of whether or not sunward magnetosphere convection terminates at the plasmopause would indicate whether or not convection is important in the formation of the plasmopause.

Although the search for the answer to these questions might seem straightforward, in practice the static nature of the models as opposed to the dynamic state of the actual magnetosphere dictate that meaningful comparisons be of a statistical nature. Unfortunately the number of particle measurements is limited, and therefore the results derived

from them have statistical uncertainties which preclude the detailed comparisons one might wish to make. One way to overcome this limitations would be to obtain additional particle measurements over more limited tilt and K_p ranges and compare then with the appropriate model. A second method of answering some of these questions that have been raised by comparisons with field models is the direct comparison of simultaneous data from different experiments for various individual events. This approach has already been profitably exploited by Frank and Gurnett (1971) and should be continued and extended.

FIGURE CAPTIONS

Figure 1 - Equatorial crossing distance and earth intersection geomagnetic latitude of the last closed field line in the noon meridian plane for dipole tilt angle of zero, plotted as a function of the median K_p value for each of the four geomagnetic field models.

Figure 2 - Contours of constant latitude (solid lines) and constant local time (dashed lines) at the earth's surface as mapped along field lines of the MF73Q field model ($K_p < 2$) to the equatorial plane (lower portion of figure) and to a tail cross section at $X = -10 R_E$ (upper portion of figure). The dipole tilt angle is zero.

Figure 3 - Same as figure 2 but for the MF73D field model ($K_p \geq 2$).

Figure 4 - Low altitude experimental determination of the polar cusp and polar cap during periods of high K_p as mapped along field lines to the equatorial plane (lower portion of figure) and to a tail cross section (upper portion of figure). The super-disturbed model ($K_p \geq 2$) was used, with tilt = 0. The solid line on the dayside correspond to the last closed field line as determined by the model.

Figure 5 - Low altitude measurements during quiet times as projected along field lines into the equatorial plane in the outer magnetosphere. The shaded region represents the polar cusp and the open circles represent the low latitude boundary of the polar cap. The dashed and solid lines emanating from the earth represent the equatorial plane projections of field lines corresponding to the 35 Kev background and smooth boundaries respectively.

Figure 6 - Low latitude electric field measurements projected to the equatorial plane with the quiet model. The shaded areas indicate regions of sunward convection.

Figure 7 - Earth intersection geomagnetic latitudes of the field lines from various local times at the synchronous orbit in the geomagnetic equatorial plane. Four field models are shown for three tilt angles.

REFERENCES

- Akasofu, S.-I., E.W. Hones, Jr., S.J. Bame, J.R. Asbridge, and A.T.Y. Lui, Magnetotail and boundary layer plasmas at a geocentric distances of $\sim 18 R_E$: Vela 5 and 6 observations, J. Geophys. Res., 78, 7257-7274, 1973.
- Aubry, Michel P., Christopher T. Russell, and Margaret G. Kivelson, Inward motion of the magnetopause before a substorm, J. Geophys. Res., 75, 7018-7031, 1970.
- Bame, S.J., J.R. Asbridge, H.E. Felthaus, E.W. Hones, and I.B. Strong, Characteristics of the plasma sheet in the earth's magnetotail, J. Geophys. Res. 72, 113-129, 1967.
- Behannon, Kenneth W., Geometry of the geomagnetic tail, J. Geophys. Res., 75, 743-753, 1970.
- Burch, J.L., Precipitation of low-energy electrons at high latitudes: effects of interplanetary magnetic field and dipole tilt angle, J. Geophys. Res., 77, 6696-6707, 1972.
- Cauffman, D.P., and D.A. Gurnett, Satellite measurements of high latitude convection electric fields, Space Sci. Rev., 13, 369-410, 1972.
- Chappell, C.R., K.K. Harris, and G.W. Sharp, The dayside of the plasmasphere, J. Geophys. Res., 76, 7632-7647, 1971.
- Choe, Joon Y., and David B. Beard, The geomagnetic field deduced from magnetopause currents, University of Kansas, Department of Physics and Astronomy preprint, 1973

- Evans, L.C., and E.C. Stone, Electron polar cap and the boundary of open geomagnetic field lines, J. Geophys. Res., 77, 5580-5584, 1972.
- Fairfield, Donald H., Average and unusual locations of the earths magnetopause and bow shock, J. Geophys. Res., 76, 6700-6716, 1971.
- Fairfield, D.H. and N.F. Ness, Configuration of the geomagnetic tail during substorms, J. Geophys. Res., 75, 7032-7047, 1970.
- Feldstein, Y.I., and G.V. Starkov, The auroral oval and the boundary of closed field lines of geomagnetic field, Planet. Space Sci., 18, 501-508, 1970.
- Frank, L.A., and D.A. Gurnett, Distribution of plasmas and electric fields over the auroral zones and polar caps, J. Geophys. Res., 76, 6829-6846, 1971.
- Freeman, J.W., Jr., C.S. Warren and J.J. Maguire, Plasma flow directions at the magnetopause on January 13 and 14, 1967, J. Geophys. Res., 73, 5719-5731, 1968.
- Fritz, Theodore A., Study of the high latitude, outer-zone boundary region for ≥ 40 -Kev electrons with Injun 3, J. Geophys. Res., 75, 5387-5400, 1970.
- Gurnett, D.A. and L.A. Frank, Observed relationships between electric fields and auroral particle precipitation, J. Geophys. Res., 78, 145-170, 1973.

- Harang, L., The mean field of disturbance of polar geomagnetic storms, Terr. Magn. Atmos. Elect., 51, 353-380, 1946.
- Heppner, J.P., Electric field variations during substorms: OGO-6 measurements, Planet Space Sci., 20, 1475-1498, 1972a.
- Heppner, J.P., Electric fields in the magnetosphere, in critical problems of magnetosphere physics, edited by E.R. Dyer, published by the IUCSTP Secretariat c/o National Academy of Science, Washington DC., 107-122, 1972b.
- Heppner, J.P., The Harang discontinuity in auroral belt ionospheric currents, in Geofys. Publ., Minneskrift for Prof. L. Harang (Eds. J. Holtet and A. Egeland) Universitetsforlaget, Oslo, 105-120, 1972c.
- Hones, E.W., Jr., J.R. Asbridge, S.J. Bame, M.D. Montgomery, S. Singer, and S.-I. Akasofu, Measurements of Magnetotail plasma flow made with Vela 4B, J. Geophys. Res., 77, 5503-5522, 1972.
- McDiarmid, I.B., and J.R. Burrows, Local time asymmetries in the high latitude boundary of the outer radiation zone for the different electron energies, Can. J. Phys. 46, 49-57, 1968.

Mead, G.D. and D.H. Fairfield, Quantitative magnetospheric models derived from spacecraft magnetometer data, submitted to J. Geophys. Res., 1973.

Roederer, J.G., Quantitative models of the magnetosphere, Rev. Geophys., 7, 77-96, 1969.

Williams, Donald J., and Gilbert D. Mead, Nightside magnetosphere configuration as obtained from trapped electrons at 1199 kilometers, J. Geophys. Res., 70, 3017-3029, 1965.

Winningham, J. David, Characteristics of magnetosheath plasma observed at low altitudes in the dayside magnetospheric cusps, in Earth's Magnetospheric Processes edited by B.M. McCormac, D. Reidel Publishing Co., Dordrecht-Holland, 68-80, 1972.

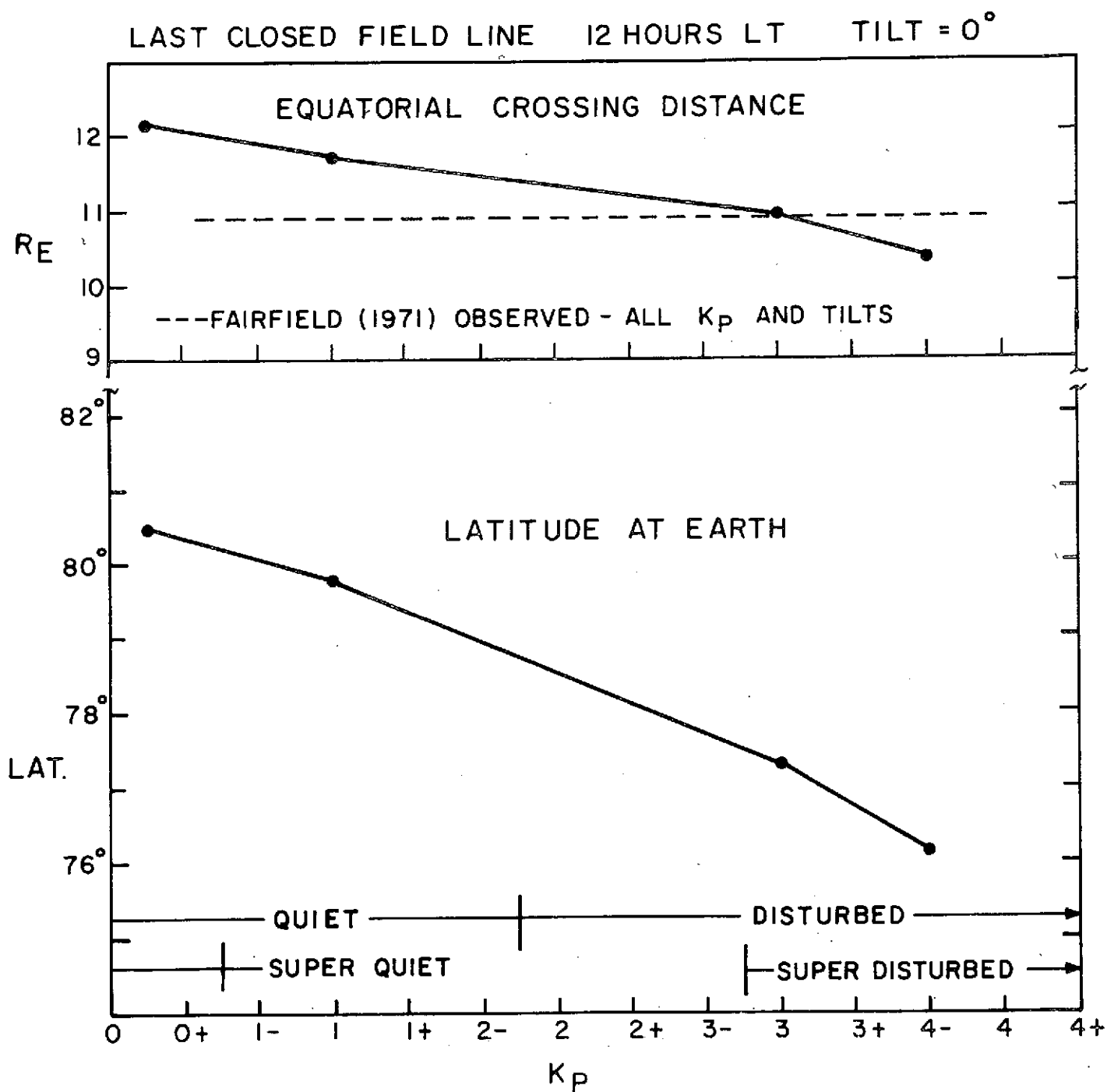


Figure 1

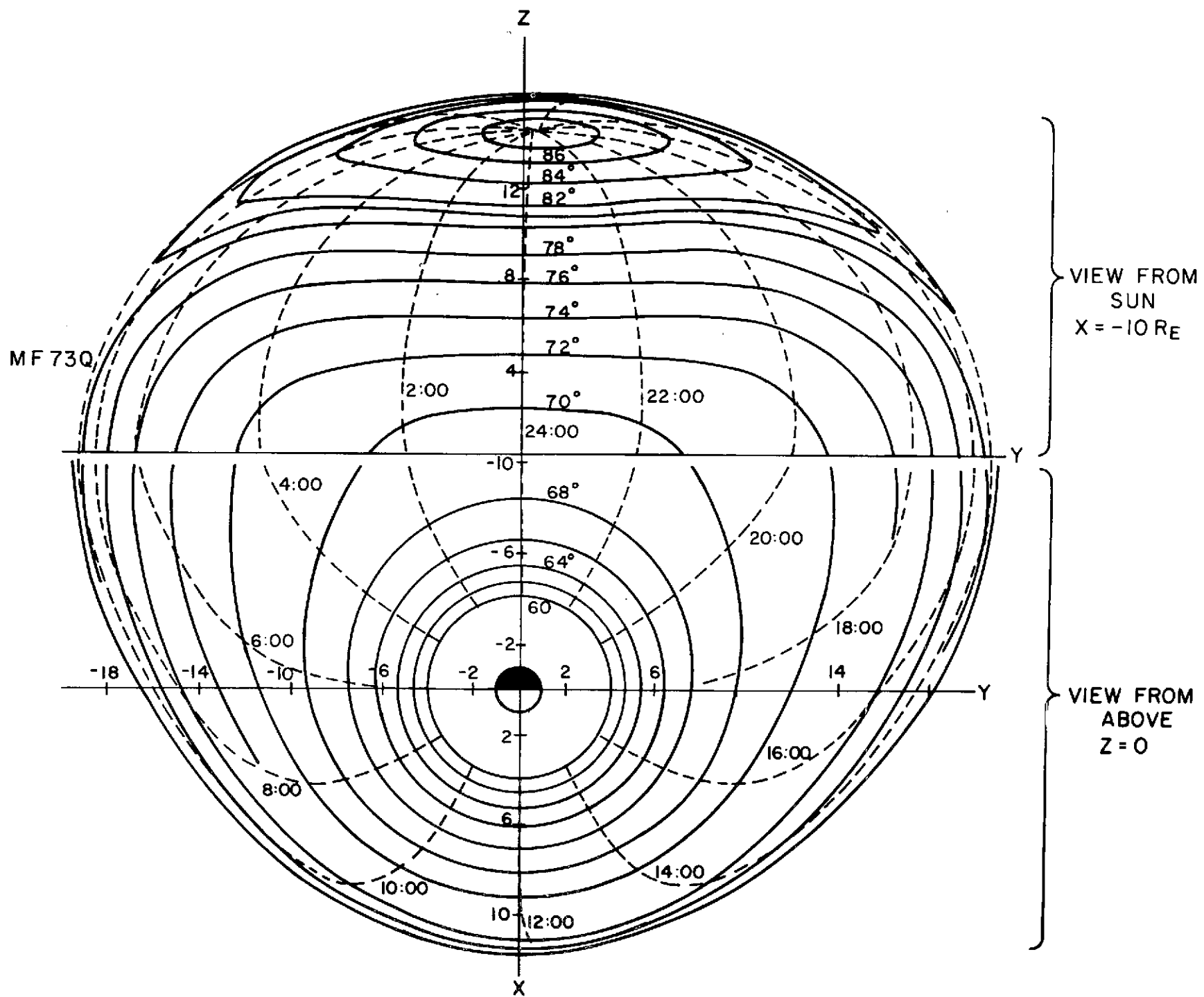
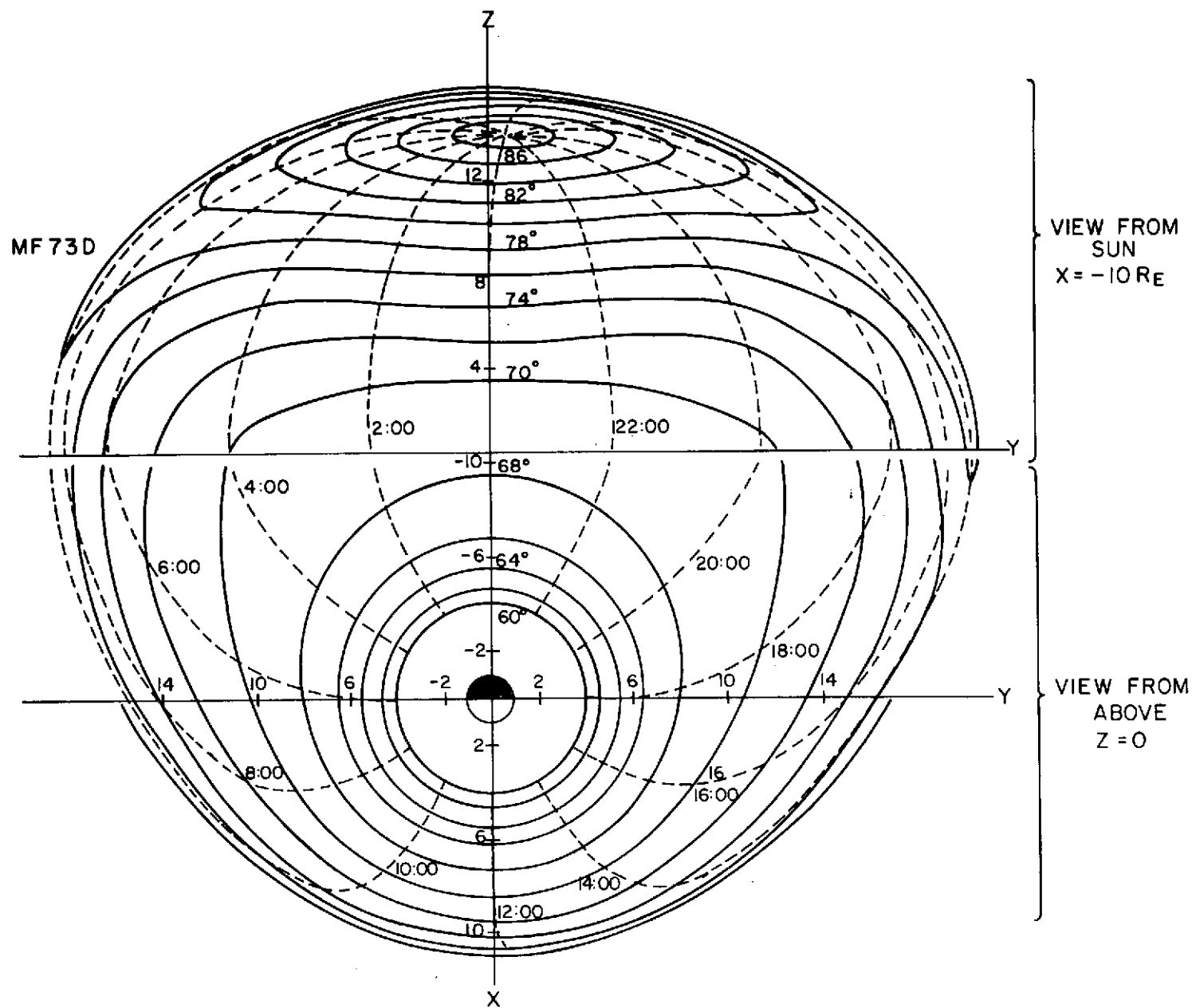


Figure 2



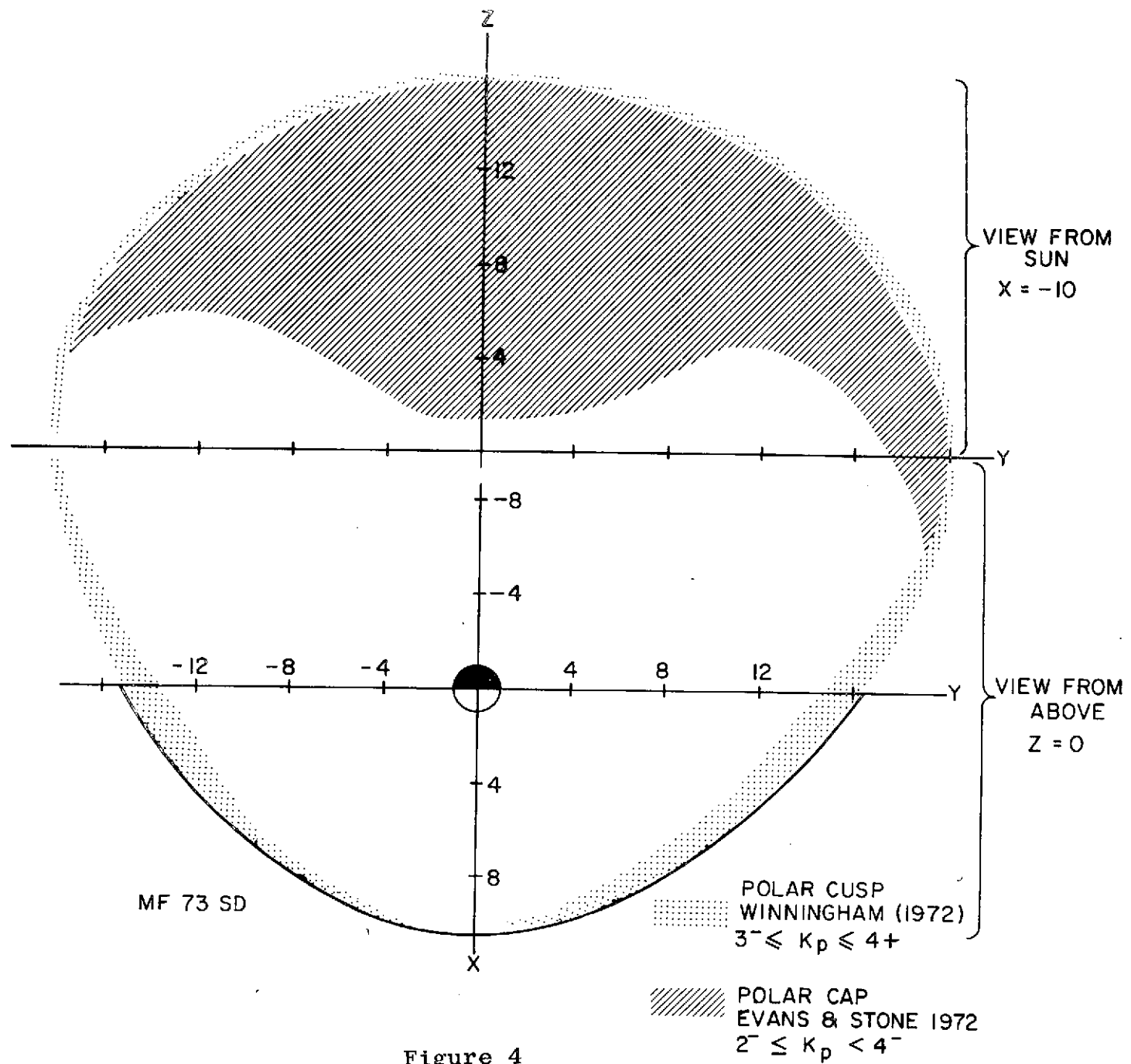


Figure 4

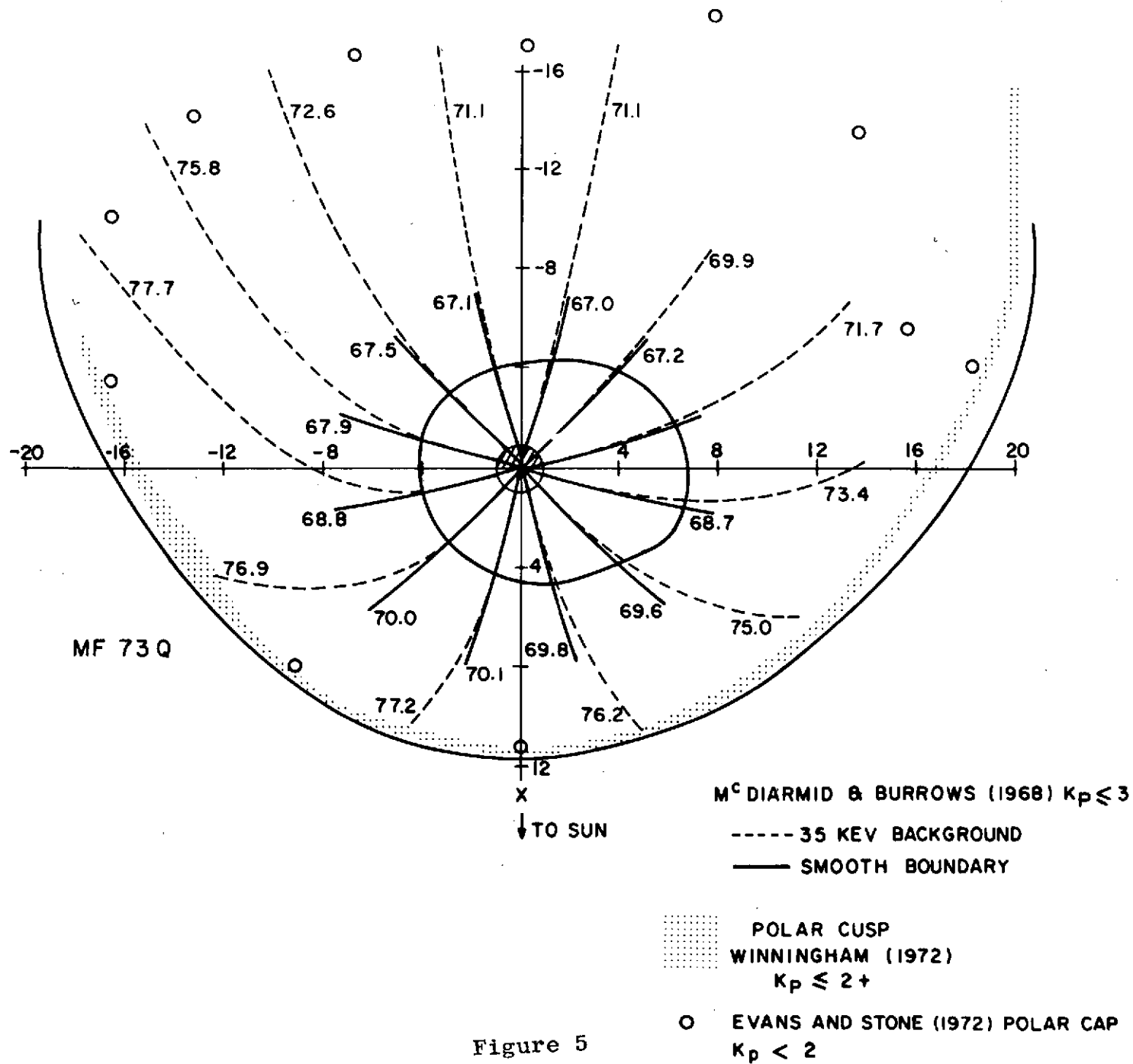
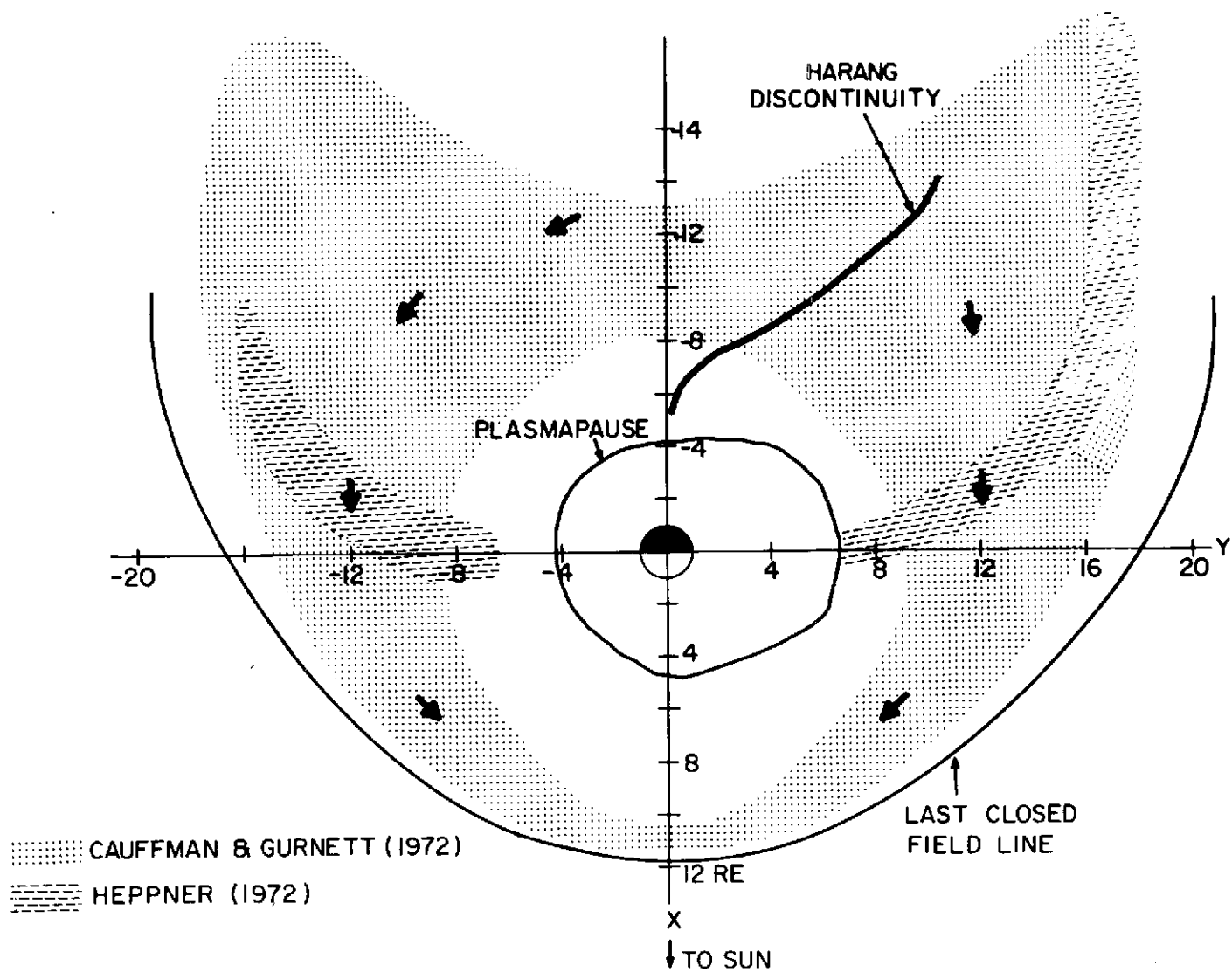
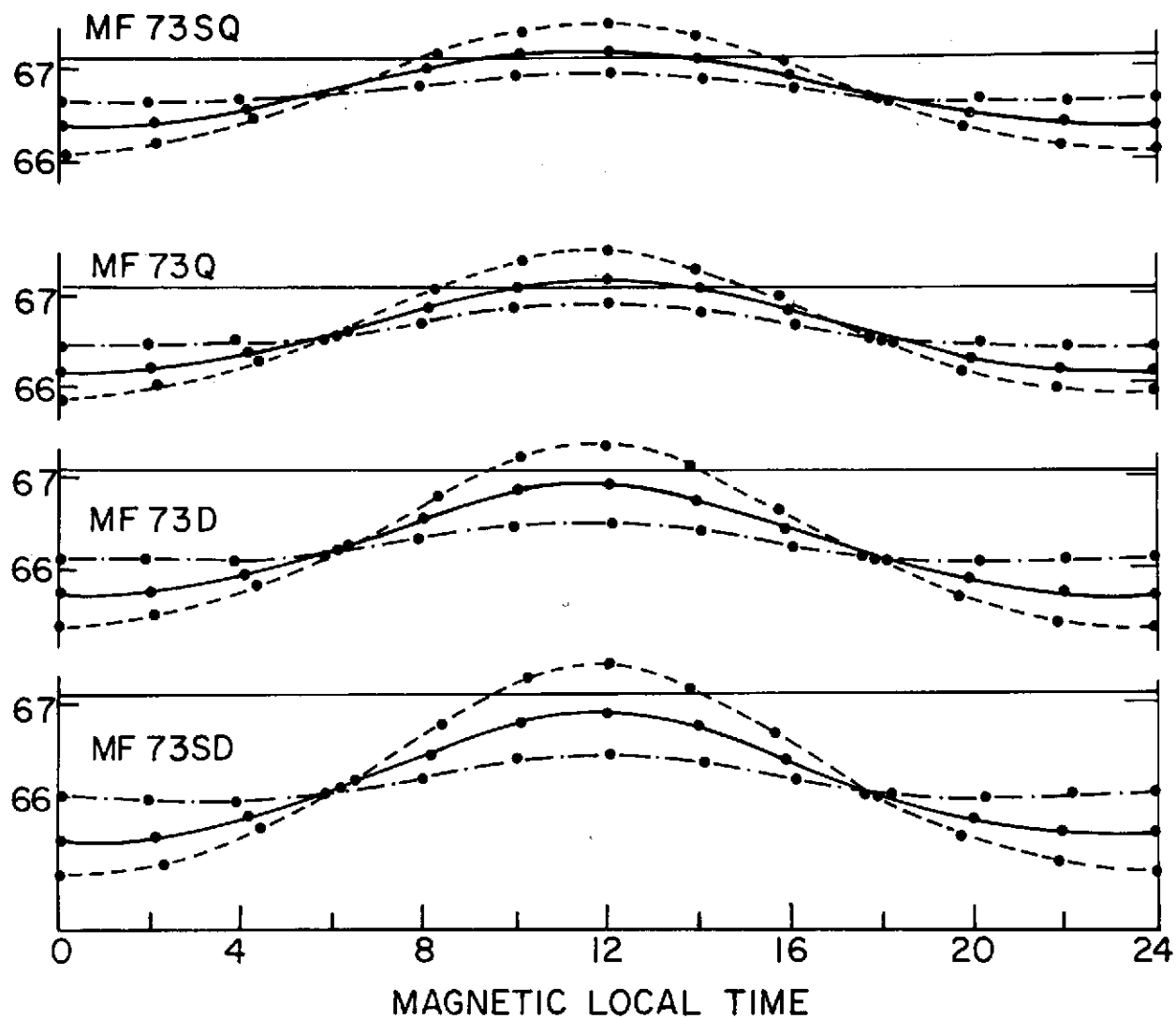


Figure 5



SUNWARD CONVECTION IN EQUATORIAL PLANE

Figure 6



— TILT = 0
 - - - TILT = 30° SUMMER
 - · - TILT = 30° WINTER

Figure 7